Final Draft
of the original manuscript:

Ghasemi, A.; Raja, V.S.; Blawert, C.; Dietzel, W.; Kainer, K.U.:
The role of anions in the formation and corrosion resistance of the plasma electrolytic oxidation coatings
In: Surface & Coatings Technology (2009) Elsevier

DOI: 10.1016/j.surfcoat.2009.09.069

The Role of Anions in the Formation and Corrosion Resistance of the Plasma Electrolytic Oxidation Coatings

A. Ghasemi[1*], V. S. Raja[2], C. Blawert[1], W. Dietzel[1], K. U.Kainer[1]

1-Institute of Materials Research, GKSS-Forschungszentrum Geesthacht GmbH, Max-Planck-St.1, D-21502 Geesthacht, Germany

2-Department of Metallurgical Engineering and Materials Science, Indian Institute of Technology Bombay, Mumbai 400 076, India

Abstract:

Combination of KOH with each of Na_2SiO_3, Na_3PO_4 and $NaAlO_2$, formed three different coating solutions to produce plasma electrolytic oxidation (PEO) coatings on the surface of AM50 magnesium alloy. The surface morphology, cross section, chemical composition, corrosion resistance and structure of each of the coatings was characterized by scanning electron microscopy (SEM), X-ray diffraction (XRD) and electrochemical impedance spectroscopy (EIS). The results showed that different anions, i.e., SiO_3^{2-}, PO_4^{3-} and AlO_2^-, influence the coating characteristics such as thickness, chemical composition and coating structure. The results showed that thicknesses of the Si-, P- and Al-coatings are 8, 4 and 1 µm, respectively. Moreover beside MgO existing in structure of all three coatings, specific phases namely Mg_2SiO_4, $Mg_3(PO_4)_2$ and $MgAl_2O_4$ were formed in the structure of the Si-P-, Al-coating, respectively. It was revealed that usage of SiO_3^{2-} instead of PO_4^{3-} or AlO_2^- led to formation of a coating layer with better corrosion protection properties. The better performance of the Si-coating compared to P- or Al-coatings is considered to be due to the fact that the thickness, the number of open pores and the resistance of the barrier layer are formed under such an optimum conditions which result in a higher corrosion resistance.

Keywords: anions, coating, plasma electrolytic oxidation, corrosion, magnesium

1. Introduction

Plasma electrolytic oxidation (PEO) is a novel process which produces a stable oxide layer on the surface of a number of metals, such as aluminium, titanium and magnesium. The layers thus generated offer a unique combination of excellent wear and corrosion resistance. Such an improvement of the corrosion and wear resistance is especially beneficial for magnesium which is highly susceptible to failures resulting from either corrosion or wear - or both. In order to develop effective coatings based on the PEO process, an understanding of the mechanisms of this process and of the parameters affecting the PEO coatings is essential.

* Corresponding author; Tel.: +49 4152 / 87-1956; fax: +49 4152 / 87-1909.
E-mail address: Ghasemia@yahoo.com / Alireza.Ghasemi@gkss.de

So far, a number of studies has been performed addressing different aspects of the PEO process and the role of effective parameters in the coating process. Thus, some publications deal with fundamentals of the formation mechanism of a coating layer in order to explain possible physical and chemical reactions occurring during the plasma formation [1-6]. Other authors examine the influence of the electrolyte [7-9], the current density [10-12] and the process time [13-15] on the final characteristics of the coatings. Several studies have also been performed to improve the corrosion resistance of the coatings. In this context, various electrolytes were employed in order to obtain high performance coatings [7,8,16,17]. A literature survey suggests that a suitable solution for the PEO process usually consists of two or more components, i.e., a hydroxide and a salt. Each component introduces different cations and anions into the solution which consequently influences the resultant coating [18].

In the present study, the role of silicate, phosphate and aluminate salts was investigated on the formation of coatings by PEO process. The combination of these salts with one or more additives is typically used to prepare a PEO coating on magnesium alloys [7-9,19-21]. The salts were chosen in such way that only one type of cations, i.e., Na^+, was introduced into the coating solution. This should allow to investigate the effect of one type of anions on the resulting characteristics of the coatings, i.e., on thickness, composition, structure and consequently on the corrosion resistance.

2. Experimental Procedure

AM50 magnesium alloy (4.4-5.5wt% Al, 0.26-0.6wt% Mn, max 0.22wt% Zn, max 0.1wt% Si, reminder Mg) specimens with dimensions of 15×15×4 mm were used as substrates for the coating process. After machining, the specimens were ground with various grades of silicon carbide paper from 800 to 2500 grade. In order to get a stable current transfer through the sample to the electrolyte, a threaded hole with a diameter of 2.5 mm was made on one edge of each sample. Then, the sample was screwed to a metallic jig which carried the current from the current source. The employed power supply had a capability to produce AC and DC currents in normal and pulsed forms up to 1000V and 3A. The samples were treated under a pulsed DC electrical source with a pulse ratio of t_{max} : t_{min} = 4 ms : 1 ms with a frequency of 50 Hz for a total duration of 5 minutes under a current density of 36.2 mA/cm^2. A duration of 5 minutes was chosen because a longer treatment in

Al containing solution would give rise to intensive and localised sparking on the surface causing damage to the coating.

Three different electrolytes were prepared with the following compositions: Na_2SiO_3 + KOH, called "Si-solution", Na_3PO_4 + KOH, called "P-solution" and $NaAlO_2$ + KOH, called "Al-solution". The concentration of each of the components was 10 g/l in distilled water. It should also be noted that throughout the manuscript the coatings obtained from these solutions are termed as Si-, P- and Al-coating, respectively.

The passivation behaviour of the substrate in the various coating solutions was also examined. To this end, the bare substrate was polarized with a scan rate of 12 mV/min from -150 to 3500 mV with respect to the open circuit potential (OCP) in each of the three coating solutions. Prior to polarization, the substrate was immersed in the respective solution for 30 min to reach a stable potential. In another test aimed at understanding the properties of the passive layer formed under the effect of SiO_3^{2-}, PO_4^{3-} and AlO_2^-anions, the bare substrates had been immersed in each of the salt solutions, i.e., Na_2SiO_3, Na_3PO_4 and $NaAlO_2$ solutions with conductivities of 18.6, 11.7 and 8.8 ms/cm, respectively, for about 525 hours. Then the samples were removed from the solution, rinsed in water and subjected to electrochemical impedance spectroscopy (EIS).

To evaluate the corrosion resistance of the PEO coatings both polarization and EIS tests were employed using fresh samples for each of these tests. Prior to the measurements, the samples were immersed in the test solution for 30 minutes to reach a stable OCP. All EIS and polarization tests were performed in 3.5 wt-% NaCl solution with a pH of 6.5. The corrosion cell consisted of a Ag/AgCl (3mol/l KCl) reference electrode, a Pt counter electrode and the coated specimen as the working electrode. The EIS equipment was set up in the frequency range between 0.1 and 10^4 Hz with amplitude of ±10 mV. The impedance data were analyzed using Zview® software.

To identify the open pores, the coated samples were immersed in a solution containing 60 g/l CH_3COOH + 5 g/l $CuSO_4$. $5H_2O$ + 15 g/l $ZnCl_2$. $7H_2O$ for 30 seconds [22]. As a result of this immersion process, copper is deposited on the alloy and decorates the open pores. A measurement of the open and total number of pores was performed using the Image Tool® software.

Scanning electron microscopy (Cambridge Stereoscan 250) was employed to observe the surface morphology of the coatings. The thickness of the coatings was measured using an eddy-current coating thickness measurement gauge (Minitest 2100, Electrophysik, Germany) and by cross-sectional images of the coatings and the substrate. To prepare the cross sections for SEM observation, the samples were ground with various grades of silicon carbide papers from 800 to 2500 grade. Subsequently, polishing, etching and gold sputtering were employed. Further, X-ray diffraction (XRD) was performed using a Siemens diffractometer D 5000 operating with Cu K_α radiation.

3. Results

3-1. Microscopy

The surface morphologies and the cross sections of the three types of coatings obtained are shown in Figs. 1 - 3. The surface of the Si-coating in Fig. 1a shows a porous structure with hole diameters ranging from 1 to 5 µm. The cross section of the coating illustrated in Fig. 1b reveals that the coating is about (8±0.7) µm thick and it is reasonably uniform in thickness.

Fig. 2a shows the surface morphology of the P-coating. It can be seen that the coating has very tiny pores with diameters below 1 µm. In contrast to the Si-coating, the cross section of the P-coating in Fig. 2b reveals a more porous structure. It appears that the pores were isolated and not connected to each other. Though the top layer of the P-coating is more porous than that of the Si-coating, it seems that there is a compact layer between the alloy surface and the porous layer. The overall coating seems to be uniform and the thickness of the P-coating is about (4±0.4) µm, i.e., it is thinner than the Si-coating.

Unlike the two other coatings, the structure of the Al-coating exhibits a remarkably different type of surface morphology. Fig. 3a reveals a non-uniform and porous nature of the coating. It can be seen that the coating thickness significantly differs from place to place. The uneven and thin cross section of the coating which can be seen in Fig. 3b further supports this observation. It should also be pointed out that, in addition to the poor nature of the coating, it is about (1±0.2) µm thick which is much thinner than the two other coatings.

Pores are typical defects that strongly influence the properties of the PEO coatings. Hence, the fraction of the oxide layer covered by the pores and the pore density were measured. The data of the open pores and the total number of pores are summarized in Table 1. The results show that 0.5%, 0.7% and 1.6% of the Si-, P- and Al-coating surfaces, respectively, were covered by open pores. To get more precise information, the density of the open pores was determined showing that the Si-, P- and Al-coatings contain 13, 17 and 33 pores/mm^2, respectively. It can be seen that while the numbers of open pores of the Si- and P-coatings are comparable, the Al-coating shows a much higher pore density.

3-2. X-ray diffraction

The phases of the PEO coatings were determined by XRD and the corresponding patterns are illustrated in Fig. 4. The JCPS files were used for comparison to index the XRD patterns. It can be seen that Mg peaks which are originated from the substrate are present in all X-ray patterns. Such an observation was also made by others who examined PEO coatings and attributed the presence of magnesium peaks to the penetration of the X-rays through the PEO coating into the substrate [23]. The patterns reveal the existence of MgO in all the coatings. Apart from MgO existing in all coatings, the specific phases, namely Mg_2SiO_4, $Mg_3(PO_4)_2$ and $MgAl_2O_4$, were detected in Si-, P-, and Al-coatings respectively.

3-3. Passivation study

The passivation behaviour of the substrate in different coating solutions was studied by the electrochemical polarization technique. The polarization curves presented in Fig. 5 show that the alloy in Si-, P- and Al-solutions behave in such way that respective passive current densities of 3.5×10^{-4}, 7.3×10^{-4} and 1.1×10^{-3} A/cm^2 arise. The data show that silicate ions have the capability to produce a more stable passive layer on the metal surface than phosphates or aluminates. As the pH of the solution also plays a key role in the passive film formation of magnesium alloys [24], the pH values of the solutions were measured showing an almost similar value of around 13 ± 0.05 for all three solutions. Therefore, the difference in passive current density and hence the difference in the properties of the passive layers should be attributed to different kind of the anions. Interestingly, in our previous studies it was shown that the resistivity of PEO coatings also depends on the resistance of the passive layer forming on the substrate in a given solution [18]. The

present study indicates that the solution producing a more stable passive layer also produces a more corrosion resistant coating.

Further examination of the nature of the passive layer was performed by immersing the bare metal in Na_2SiO_3, Na_3PO_4, $NaAlO_2$ solutions. Subsequently, the resistance of the passive layer formed was measured by EIS technique. The results shown in Fig. 6 indicate that the layer which was formed in Na_2SiO_3 solution had a higher impedance value than that of the Na_3PO_4 solution and that of the latter is still higher than that formed in the $NaAlO_2$ solution.

3-4. Electrochemical corrosion studies

The corrosion resistance of the PEO coatings was evaluated by both potentiodynamic polarization and EIS methods. Morphology of the corrosion attack and polarization plots of the coated specimens are shown in Figs. 7 and 8, respectively. As can be seen in the Fig. 8, the cathodic polarization curves of the coatings exhibit a diffusion limited current density, i_L. The i_L values of the coated alloy decrease in the order Al-coating > P-coating > Si-coating. Notably, the reduction of i_L is responsible for the variation in corrosion potential, E_{corr}, and corrosion current density, i_{corr}, of the alloy since these values follow the same trend as that of i_L. Both i_{corr} and corrosion rate values of the coatings are shown in Table 2. The data clearly show that the Si-coating exhibits a much lower corrosion rate than the P- and the Al-coatings. However, it is also seen that no retarded dissolution of magnesium occurred during the anodic polarization.

The electrochemical corrosion behaviour of the untreated AM50 alloy and the coatings in 3.5% NaCl are shown in figs 9-12. It is seen that the Nyquist and Bode plots of the coatings show a good agreement with the polarization results. The impedance data of the Bode plots show that the highest polarization resistance, R_P, of the PEO coatings belongs to the Si-coating with 2.3×10^6 $\Omega\cdot cm^2$ while the P- and Al-coatings have a polarization resistance of 3.1×10^5 and 1.4×10^3 $\Omega\cdot cm^2$, respectively.

4. Discussion

As mentioned before, morphology, thickness, chemical composition and structure are considered to be the major parameters influencing the final performance of the PEO

coating. The behaviour of these parameters with respect to the three different anions is discussed in the following sections;

4-1. Surface morphology

Figs. 1-3 clearly reveal that the pores in the surface morphology of the Si-coating are larger than those of the P- and the Al-coating. The different surface morphology of the various coatings may be related to the dissimilar characteristics of the micro-sparks, such as size and number of sparks occurring during the PEO process. It was reported that the surface of the coating gets coarser and rougher as the process proceeds and the oxide layer gets thicker [7,25-28]. Essentially in a thicker layer of the coating, higher energy is required for the current to pass through the coating. Under this condition, the current is localized at weak points of the layer formed to find its way through the coating. This is the reason why the number of sparks decreases but their size increases as the layer gets thicker. In fact, an increase in diameter of the discharge channels is the way how the process compensates the reduction in number of the channels [26]. Hence, the size and the number of sparks are affected by the thickness of the layer. It was also reported that the number of sparks during the PEO process in phosphate electrolytes is higher than that of silicate electrolytes, resulting in a higher number of pores after cooling of the discharge channels [7].

As mentioned in the previous section, the beneficial effect of SiO_3^{2-} anions in comparison to that of the phosphate and aluminate anions lies in the fact that the former enhance the growth rate of the PEO coating. It is seen that in a given time, the thickness of the Si-coating reaches to higher value than those of P- and Al-coatings. This consequently gives rise to the bigger sparks occurring on the surface. This may explain the formation of larger holes on the surface of the Si-coating in comparison to those of P- and Al-coatings.

4-2. Cross section

The SEM images show that the cross sections of the three types of coatings differ from one another. For instance, it is seen that unlike the Si-coating, the cross section of the P-coating shows a more porous structure. According to Curran et al. [23], the porosity forms because of oxygen evolution during the PEO process. As the life time of the discharges is very short, approximately 10µs, the evolved oxygen seems to be trapped in the molten material. In spite of the initial expectation that the pores deteriorate the corrosion resistance of the

coating these defects can also provide the proper condition for a stable growth of the oxide layer while it is forming.

It should be kept in mind that the layers have the characteristics of a dielectric material. Therefore, the coating process would be stopped if a defect free layer formed on the surface [23]. The presence of open pores provides a proper route for the electrolyte to penetrate through the thickness of the coating. Hence, fine scale discharges could occur across a relatively thin barrier near the substrate interface, and as a result, the inner defects could be recovered and a compact layer would form on the surface. Sundararajan et al. suggest that the discharge channels have a finite life, i.e., that the discharge channels are continuously formed and closed throughout the coating process [26].

Therefore, as the solution can penetrate easier into the discharge channels through the larger openings compared to the narrow ones, the holes with larger diameters could be more beneficial for the formation of the coating. This may explain why the Si-coating has a coarse surface morphology with big holes but its cross section shows less evidence of porosity or defects. It could also explain what happens to the surface morphology and cross section of the P-film; As Figs. 2a and 2b show the openings on the surface of the P-coating (unlike the Si-coating) are so fine and small that the coating solution can not easily penetrate to the discharge channels. Therefore, some holes and defects may form in the cross section of the coating. In the case of the Al-coating the cross section of the coating seems to be too thin to show apparent defects, although the surface morphology proposes a fine porous structure.

The measurement of the open pores also shows a good consistency with the cross section results. It can be seen that the Si-coating with an open pore density of 13 pores/mm^2 and a surface coverage of 0.5% had the lowest amount of the open pores. The open pore data of the P-coating with ~17 pores/mm^2 and ~0.7% coverage of the surface show higher values than Si-coating. The highest amount of open pores was observed for the Al-coating where the density of pores was 33 pores/mm^2 and the percentage of the surface coverage was 1.6%. The results are also in good agreement with the corrosion resistance data, where i_{corr} of the Si- , P- and Al-coatings is about 3.2×10^{-06}, 9.5×10^{-04} and 8.7×10^{-03} mA/cm^2, respectively. The data indicate that a lower number of open pores or likewise a higher coverage of the surface leads to a higher corrosion resistance of the coatings.

4-3. Thickness

The cross sections of the coatings show that the thickness of the Si-, P- and Al-coating is about 8, 4 and 1µm, respectively. Since all the coatings were prepared within a period of 5 minutes, the growth rate of the Si-, P- and Al-coating turns out to be 1.6, 0.8 and 0.2 µm/min, respectively. This gives a supportive evidence of the beneficial influence of the silicate anions on the growth rate of the PEO coating compared to that of phosphate or aluminate anions. Different literature also pointed out to the beneficial effect of silicate on the growth rate of PEO coatings. [26,29,30].

An earlier investigation of PEO coatings showed that the structure of a PEO coating is composed of an inner barrier layer and an outer porous layer [18]. While the porous layer forms as a result of the plasma interaction between the metal and the electrolyte, the barrier layer at the bottom of open pores forms due to the reaction of the electrolyte and the substrate. Hence, the electrochemical properties of the barrier layer substantially depend on the interaction between the metal surface and the electrolyte species. Duan et al. also showed that the anions have a direct influence on the thickness and morphology of the PEO coating [8].

The formation of the barrier layer is a consequence of the reaction between metal ions, in this case Mg^{2+}, and anions existing in the solution. Therefore, formation of a coating layer requires the anodic dissolution to provide metal ions for subsequent reactions with the anions leading to layer formation. The “rate of anodic dissolution” and the “rate of film formation” are two opposing factors which reversely influence the final thickness of the PEO coating. Essentially the coating starts to grow as the rate of the film formation gets higher than the dissolution rate of the substrate [3].

From the “anodic dissolution” point of view, the study of the passive layer on the metal surface, Fig. 5, showed that SiO_3^{2-} ions form a more stable passive layer on the metal surface in the initial step of the PEO process compared to that of the phosphate or aluminate ions. The passivation study by EIS illustrated in Fig. 6 also indicates that the layer resulted from the Na_2SiO_3 solution had a higher impedance value than those resulting from the Na_3PO_4 and $NaAlO_2$ solutions, respectively. The formation of a more stable passive layer in Si-solution obviously can prevent further dissolution of the substrate and subsequently less anodic dissolution.

Another evidence of the formation of a more stable oxide layer in the Si-solution could be the final voltage of the PEO process. Several authors showed that the increase of the voltage during the PEO process is due to the resistance of the oxide layer against the passing current [3,7]. This aspect can be examined by measuring the final voltage of the PEO process. The final voltages of the Si-, P- and Al-coatings were 376, 367 and 244 V, respectively. The higher final voltage of the Si-coating indicates that the Si-layer is more stable than the two others. The thickness of the corresponding coatings also shows a direct relation to the final voltages of the PEO process, which is in good agreement with the literature [31,32].

Further, the effect of conductivity on the film formation process was examined. Guo et al. reported that the rate of film formation increased when anions with higher conductivity were introduced to the coating solution [33]. The conductivity of 10g/l of the Na_2SiO_3, Na_3PO_4 and $NaAlO_2$ solutions measured in this work were about 18.6, 11.7 and 8.8 mS/cm, respectively. It shows that the Si-solution had the highest and the Al-solution has the lowest conductivity. Therefore, the high rate of film formation of the Si-coating may be attributed to a higher conductivity of the solution. The same argument should be valid for the low growth rate of the coating in the Al-solution. Therefore, a low anodic dissolution and a high rate of film formation can explain why the Si-coating gets thicker than the two other coatings.

4-4. Chemical composition

The chemical composition of the PEO coating is among the parameters which influence the corrosion resistance of the final coating [7,9,34-36]. So a phase analysis of the coatings can provide valuable information regarding the performance of the coatings.

The XRD results showed that the anions are involved in the formation process and produce different phases in the coatings. Apart from MgO which is commonly detected in the coatings, depending on the electrolyte type, specific phases form during the coating process. The results of the present study show that Si-, P- and Al-solutions respectively introduce Mg_2SiO_4, $Mg_3(PO_4)_2$ and $MgAl_2O_4$ phases into the coating structure. The formation of these phases could be based on the following reactions:

$2Mg^{2+} + SiO_3^{2-} + 2OH^- = Mg_2SiO_4 + H_2O$ (1) [37]

$3Mg^{2+} + 2PO_4^{3-} = Mg_3(PO_4)_2$ (2) [38]

$Mg^{2+} + 2AlO_2^- = MgAl_2O_4$ (3) [13].

Liang et al. compared the corrosion resistance of two coatings. The first was mainly composed of MgO and Mg_2SiO_4, and the second one of MgO. Although the results showed that both coatings provided effective corrosion protection, the coating containing Mg_2SiO_4 showed a better corrosion resistance [7]. A comparison of the corrosion resistance of the coatings which are composed of MgO and $MgAl_2O_4$ also showed that a higher amount of $MgAl_2O_4$ increased the corrosion resistance of the PEO coating [21]. Other studies have additionally reported the beneficial effect of stable phases such as Mg_2SiO_4 [34,36] $Mg_3(PO_4)_2$ [8] and $MgAl_2O_4$ [13,35] to improve the corrosion resistance of PEO coatings. Therefore, one of the major roles of the anions seems to be an influence on the chemical composition of the coatings leading to different corrosion performance of the coatings.

To determine the fraction of the phases, the coatings were characterized by considering the intensity of the main peaks of each phase in the XRD patterns. The ratio of the intensities was used to calculate the relative variation of the phases existing in the coating. Thus, the ratios of I_{MgO} / I_{Mg}, $I_{Mg_2SiO_4} / I_{MgO}$, $I_{Mg_3(PO_4)_2} / I_{MgO}$ and $I_{MgAl_2O_4} / I_{MgO}$ were determined. The results show that the ratio of I_{MgO}/I_{Mg} is 0.192, 0.25 and 0.037 for Si-, P- and Al-coating, respectively. It can be seen that the Al-coating has the lowest ratio which could be because of the low thickness of the coating. On the other hand, although the P-coating had a lower thickness compared to the Si-coating, it had a higher ratio of I_{MgO}/I_{Mg} which might indicate that a higher fraction of the P-coating consisted of MgO compared to that of the Si-coating. The calculations yield $I_{Mg_2SiO_4} / I_{MgO}$ = 1.03, $I_{Mg_3(PO_4)_2} / I_{MgO}$ = 0.21 and $I_{MgAl_2O_4} / I_{MgO}$ = 1.87 for the Si-, P-, Al-coating, respectively. It is seen, although Mg_2SiO_4 and MgO were forming almost in equal fraction in the Si-coating, in the case of the P-coating a lower amount of $Mg_3(PO_4)_2$ was present in the coating structure compared to that of MgO. This confirms that a higher fraction of the P-coating was composed of MgO. Considering the ratios of the Al-coating may lead to the conclusion that the fraction of $MgAl_2O_4$ in this coating is higher than that of MgO.

4-5. EIS study

4-5-1. Si-coating

The electrochemical properties of the coatings were examined using electrical equivalent circuits representing various elements of the coatings. The equivalent circuits employed for curve fitting of the Si-, P- and Al-coatings are illustrated in Fig. 13. It should be noted that different combinations of elements (such as resistor, capacitor, and Warburg diffusion) in different sequences (i.e. parallel, series) were checked. Among the different combinations, the indicated equivalent circuits gave the best fitting results with the lowest error. The proposed equivalent circuit for the Si-coating consisting of two time constants suggests two different resistances in the coating, namely the coating layer and a passive layer. R_S, R_1 and R_2 represent the resistance of the solution, the coating and the passive layer, respectively. CPE_1 and CPE_2 represent the capacitances of the coating and the passive layer, respectively.

The experimental and fitted results are illustrated in Fig. 10. Moreover the corresponding data are listed in the Table 3. As Fig. 1a conveys, the coating surface is very porous and consists of big holes. Therefore, R_1 attains a low value. On the other hand, the cross section of this coating in Fig. 1b shows a relatively uniform layer on top of the metal surface. According to the obtained data the magnitude of R_1 and R_2 are 3.2×10^4 and 5.6×10^6 $\Omega\cdot cm^2$, respectively. A low R_1 and a much higher R_2 value point to the fact that the porous layer of the coating was not able to provide high resistance against the corrosion and the total resistance of the coating was mainly derived from the passive layer which was laid directly onto the metal surface, acting as a barrier against the corrosive electrolyte to reach the substrate.

4-5-2. P-coating

Fig. 13-b shows the equivalent circuit giving the best fit for the impedance data of the P-coating. It is clear that the equivalent circuit has an additional Warburg element compared to that of the Si-coating. The presence of the Warburg element which is an evidence for a diffusion controlled process in the P-coating can be explained as following; At the corrosion potential, the rate of dissolution of Mg alloy is very low in the Si-coating due to a more protective layer. Because the corrosion rate (occurring at the interface) is very low, a faster diffusion is not required to sustain the corrosion rate, and so it is not diffusion controlled. On the other hand, the corrosion rate of the Mg alloy is much higher in the P-

coating condition. Therefore, long range diffusion is required to sustain the corrosion rate. In other words, it can be said that the difference between R_1 and R_2 is much higher in the Si-coating than in the P-coating which could be because of the higher number of open pores in the P-coating.

4-5-3. Al-coating

The fitting results for the Al-coating presented in Fig. 12 show a depressed Nyquist curve in the high and medium range of frequencies. The depressed semicircle of the Nyquist curve can be attributed to a quite rough and uneven surface morphology of the coating [39,40]. In the low frequency range, however, the curve attains negative values forming a curve known as an inductive loop. This loop can be attributed to relaxation reactions (decomposition of metal to ions leading to the formation of corrosion products) and then to the adsorption of electro-active species of the electrolyte. These processes lead to localized corrosion followed by the formation of pits on the surface [41,42].

The low thickness and the high number of open pores in the Al-coating make the layer so weak and porous that the electrolyte passes through the thickness within a short time and easily reaches the substrate. As the diffusion of H_2O molecules through the layer is easier than that of salts such as NaCl, the interaction between H_2O and the metal surface might be the first reaction taking place according to equations (4) and (5) [41]:

$$Mg + 2H_2O = Mg(OH)_2 + H_2 \quad (4)$$

$$MgO + H_2O = Mg(OH)_2 \quad (5)$$

As a result, corrosion products such as Mg^{2+} and $Mg(OH)_2$ form on the metal surface. These intermediate products have the ability to adsorb the electro-active species of the electrolyte which in the case of using a NaCl electrolyte could be Cl^- or H^+ [43-45]. The presence of such aggressive species leads to localized corrosion of the substrate which is usually detected as pits.

The equivalent circuit shown in Fig. 13c generates a curve which fits to the experimental data with the lowest error. The circuit consists of two time constants together with an inductor (L) and a resistor (R_L) which are parallel with one of the time constant components. The inductor in the equivalent circuit represents the negative loop of the

Nyquist curve. It should be pointed out that in spite of the fact that the Al-coating exhibits a much higher corrosion rate than the P-coating, the Nyquist plot does not show a Warburg behaviour. This is primarily due to the fact that the so-called porous and compact layers do not offer any resistance to the flow of ions and hence of the current.

5- Conclusions

1- The results showed that the surface morphologies and cross sections of the coatings were affected by the anions. The Si-coating had a rough and porous surface morphology but less pores in the cross section. The P-coating had a fine surface morphology including tiny pores. The cross section of the coating also contained some pores. The Al-coating had a non-uniform and porous structure, and its cross section was uneven and thin. The different thicknesses of the Si-, P- and Al-coating which were about 8, 4 and 1 µm, respectively, show that different anions can have an influence on the formation rate of the layer.

2- The presence of SiO_3^{2-} anions in the Si-solution produced a more stable passive layer on the AM50 magnesium alloy compared to that of PO_4^{3-} in the P-solution. Moreover the latter one produced a more stable passive layer compared to that of AlO_2^- in the Al-solution.

3- The results showed that the anions directly contributed to the coating formation process. Apart from MgO which is a common phase in the coatings, specific phases, i.e. Mg_2SiO_4, $Mg_3(PO_4)_2$ and $MgAl_2O_4$, resulted from the Si-, P- and Al-solutions, respectively.

4- Based on the curve fitting results, the structures of the Si-, P- and Al-coating can be represented by two time constants, Warburg and inductive elements, respectively. These results indicated that the corrosion process of the P-coating was controlled by diffusion but that of the Al-coating led to the local corrosion and pits.

5- The presence of SiO_3^{2-} anions in the coating solution seems to be more beneficial for the corrosion resistance of the PEO coating than that of PO_4^{3-} or AlO_2^-. It seems that parameters such as thickness, composition and structure of the coating in the Si-solution form in such an optimal way that the coating shows a higher corrosion resistance than the P- and the Al-coating.

6- Acknowledgements

The authors gratefully acknowledge the technical supports extended by Mr. U. Burmester and V. Heitmann. One of the authors (A.G.) expresses his sincere thanks for the financial support received by Helmholtz-DAAD Fellowship program.

7- References

[1] N. Sato, Electrochim. Acta, 16 (1971) 1683-1692.

[2] N.F. Mott, R.J.W. Tobin, Electrochim. Acta, 4 (1961) 79-107.

[3] L.O. Snizhko, A.L. Yerokhin, A. Pilkington, N.L. Gurevina, D.O. Misnyankin, A. Leyland, A. Matthews, Electrochim. Acta, 49 (2004) 2085-2095.

[4] M.R. Ok, E.Y. Kang, J.H. Kim, Y.S. Ji, C.W. Lee, Y.J. Oh, K.T. Hong, Mater. Sci. Forum, 539-543 (2007) 1258-1263.

[5] M. D. Klapkiv, Mater. Sci., 35 (1999) 279-282.

[6] A.G. Rakoch, V.V. Khokhlov, V.A. Bautin, N.A. Lebedeva, Y.V. Magurova, I.V. Bardin, Prot. Met., 42 (2006) 158-169.

[7] J. Liang, L. Hu, J. Hao, Appl. Surf. Sci., 253 (2007) 4490-4496.

[8] H. Duan, C. Yan, F. Wang, Electrochim. Acta, 52 (2007) 3785-3793.

[9] H.Y. Hsiao, H.C. Tsung, W.T. Tsai, Surf. Coat. Technol., 199 (2005) 127-134.

[10] Z. Shi, G. Song, A. Atrens, Corros. Sci., 48 (2006) 1939-1959.

[11] C.B. Wei, X.B. Tian, S.Q. Yang, X.B. Wang, R.K.Y. Fu, P.K. Chu, Surf. Coat. Technol., 201 (2007) 5021-5024.

[12] S.Y. Chang, Y.L. Kim, B.H. Song, J.H. Lee, Solid State Pheno., 124-126 (2007) 767-770.

[13] Y. Ma, X. Nie, D.O. Northwood, H. Hu, Thin Solid Films, 494 (2006) 296-301.

[14] C. Blawert, V. Heitmann, W. Dietzel, H.M. Nykyforchyn, M.D. Klapkiv, Surf. Coat. Technol., 200 (2005) 68-72.

[15] Y. Ma, H. Hu, D. Northwood, X. Nie, J. Mater. Proce. Technol., 182 (2007) 58-64.

[16] Q. Cai, L.Wang, B. Wei, Q. Liu, Surf. Coat. Technol., 200 (2006) 3727-3733.

[17] Y. Ma, X. Nie, D.O. Northwood, H. Hu, Thin Solid Films, 469-470 (2004) 472-477.

[18] A.Ghasemi, V.S.Raja, C.Blawert, W.Dietzel, K.U.Kainer, Surf. Coat. Technol., 202 (2008) 3513-3518.

[19] L. Chai, X. Yu, Z. Yang, Y. Wang, M. Okido, Corros. Sci., (2008), doi: 10.1016/ j.cor sci. 2008.08.038.

[20] S. Verdier, M. Boinet, S. Maximovitch, F. Dalard, Corros. Sci., 47 (2004) 1429.

[21] J. Liang, B. Guo, J. Tian, H. Liu, J. Zhou, W. Liu, T. Xu, Surf. Coat. Technol., 199 (2005) 121-126

[22] W. Dietzel, M. Klapkiv, H. Nykyforchyn, V. Posuvailo, C. Blawert, Mater. Sci., 40 (2004) No. 5.

[23] J.A. Curran, T.W. Clyne, Acta Mater., 54 (2006) 1985-1993.

[24] Magnesium and magnesium alloys, ASM specialty hand book (1999) 194.

[25] W.C. Gu, G.H. Lv, H. Chen, G.L. Chen, W.R. Feng, S.Z. Yang, Mater. Sci. Eng., A 447 (2007) 158-162.

[26] G. Sundararajan, L.R. Krishna, Surf. Coat. Technol., 167 (2003) 269-27.

[27] Y.M. Wang, T.Q. Lei, B.L. Jiang, L.X. Guo, Appl. Surf. Sci., 233 (2004) 258.

[28] B.H. Long, H.H. Wu, B.Y. Long, J.B. Wang, N.D. Wang, X.Y. Lu, Z.S. Jin, Y.Z. Bai, J. Phys. D: Appl. Phys., 38 (2005) 3491-3496.

[29] A.A. Voevodin, A.L. Yerokhin, V.V. Lyubimov, M.S. Donley, J.S. Zabinski, Surf. Coat. Technol., 86-87 (1996) 516-521.

[30]A.L. Yerokhin,T, A. Shatrov, V. Samsonov, P. Shashkov, A. Pilkington, A. Leyland, A. Matthews, Surf. Coat. Technol., 199 (2005) 150-157.

[31] V.I. Birss, S.J. Xia, R. Yue, R.G. Rateick, J. Electrochem. Soc., 151 (2004) B1-B10.

[32] S.J. Xia, R. Yue, R.G. Rateick, V.I. Birss, J. Electrochem. Soc., 151 (2004) B179-B187.

[33] H.F. Guo, M.Z. An, Appl. Surf. Sci., 246 (2005) 229-238.

[34] H. Luo, Q. Cai, B. Wei, B. Yu, D. Li, J. He, Z. Liu, J. Alloys Compd., 464 (2008) 537-543.

[35] O. Khaselev, D. Weiss, J. Yahaloma, J. Electrochem. Soc., 146 (5) (1999) 1757-1761.

[36] H. Fukuda,Y. Matsumoto, Corros. Sci., 46 (2004) 2135-2142.

[37] H. Duan, C. Yan, F. Wang, Electrochim. Acta, 52 (2007) 5002-5009.

[38] G.H. Lv, H. Chen, W.C. Gu, L. Li, E.W. Niu, X. H. Zhang, S.Z. Yang, J. Mater. Process. Technol., 208 (2008) 9-13

[39] S.C. Chung, J.R. Cheng, S.D. Chiou, H.C. Shih, Corros. Sci., 42 (2000) 1249-1268.

[40]R.cottis, S.turgoose, Electrochemical Impedance and Noise, NACE (1999) 45.

[41] H. Duan, K. Du, C. Yan, F. Wang , Electrochim. Acta, 51 (2006) 2898-2908.

[42] L. Kouisni, M. Azzi, F. Dalard, S. Maximovitch, Sur. Coat. Technol., 192 (2005) 239-246.

[43] S.S. Rehim, H.H. Hassan, M.A. Amin, Corros. Sci., 46 (2004) 5-25.

[44] L. Garrigues, N. Pebere, F. Dabosi, Electrochim. Acta, 41 (1996) 1209-1215.

[45]H. J. W. Lenderink, M. V. D. Linden, J. H. W. De Wit, Electrochim. Acta, 38 (1993) 1989-1992.

List of figures:

List of tables:

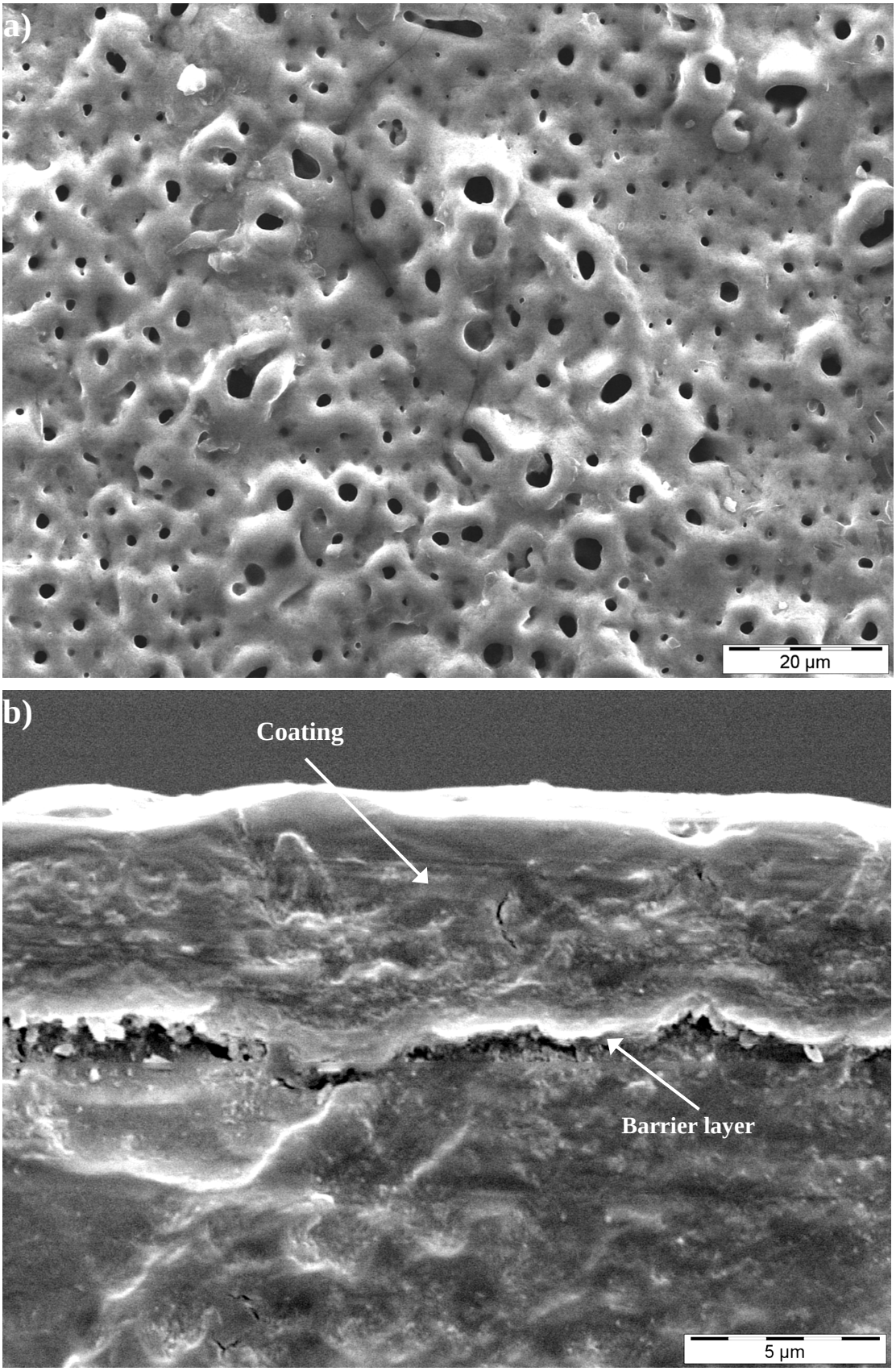

Fig. 1: (a) Surface morphology and (b) cross section of a Si-coating

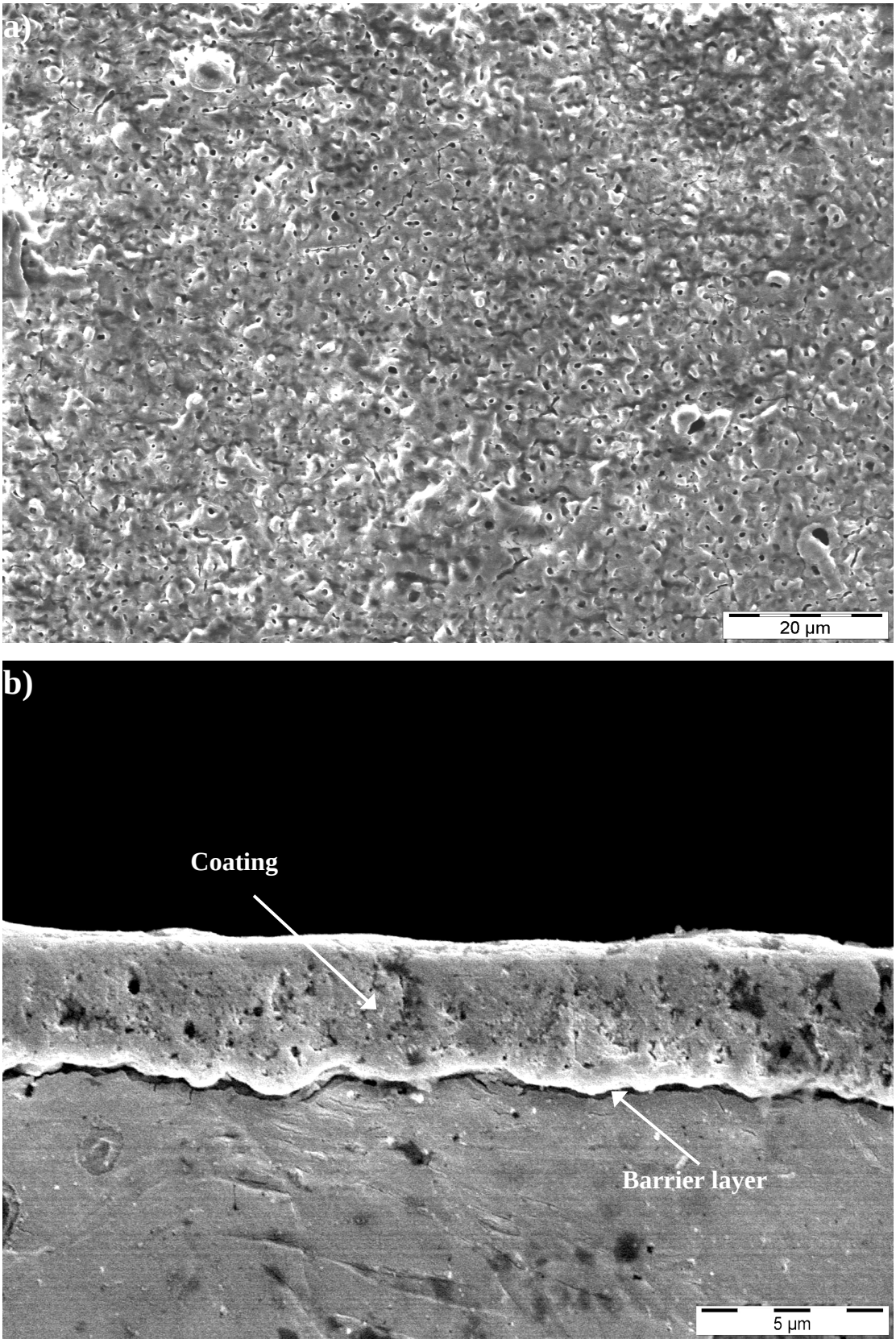

Fig. 2: (a) Surface morphology and (b) cross section of a P-coating.

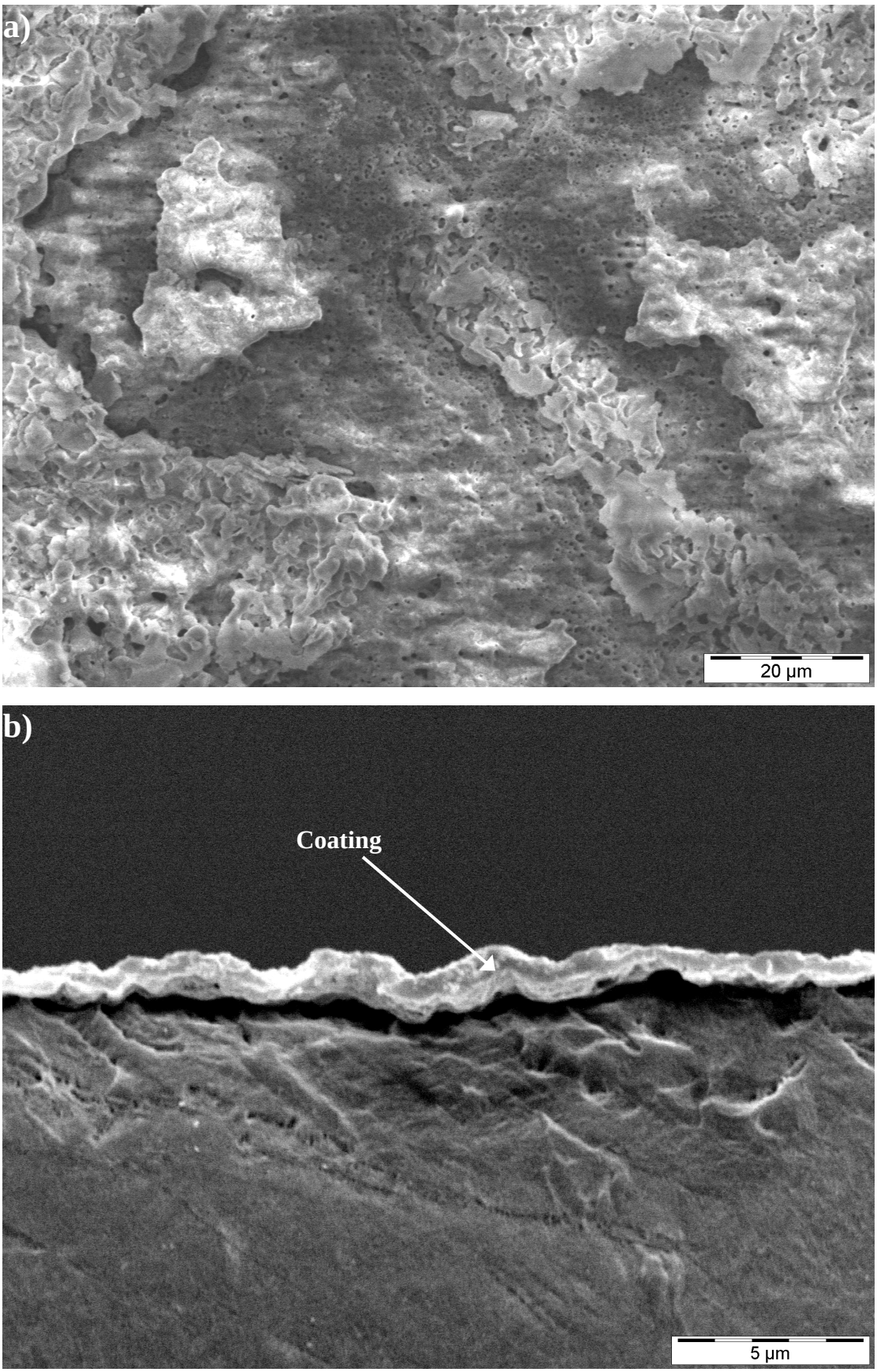

Fig. 3: (a) Surface morphology and (b) cross section of an Al-coating.

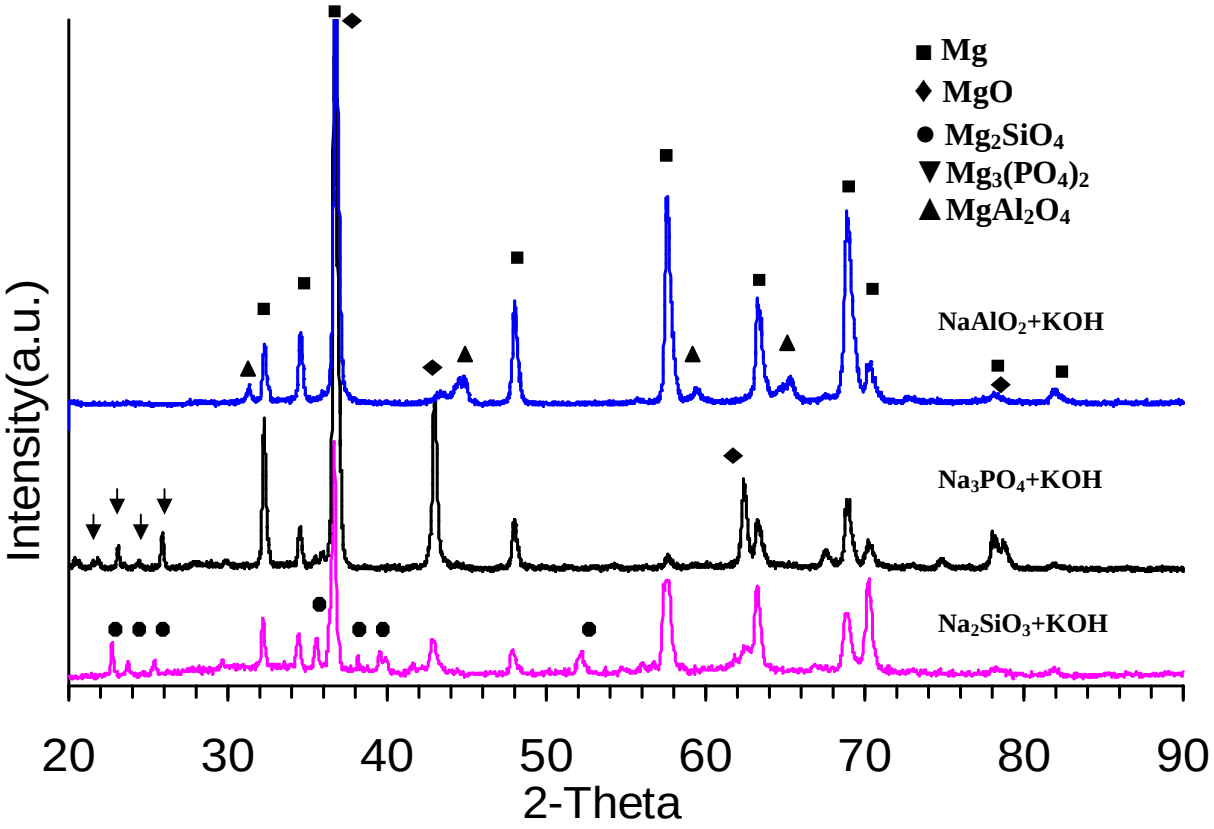

Fig. 4: XRD patterns to determine the chemical composition of the PEO coatings.

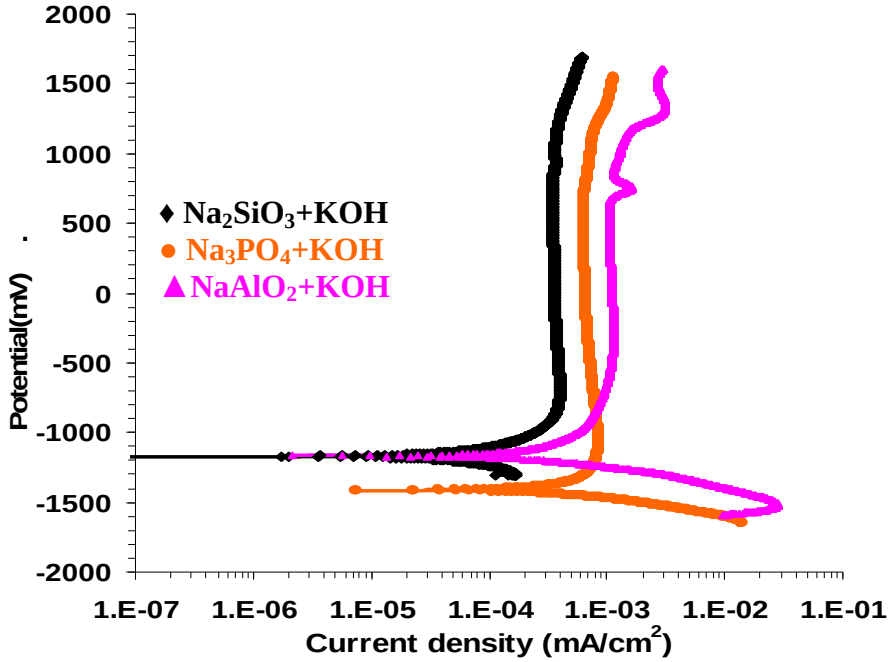

Fig. 5: Polarization curves of AM50 alloy by Na_2SiO_3+KOH, Na_3PO_4+KOH and $NaAlO_2$+KOH with scan rate of 12 mV/min.

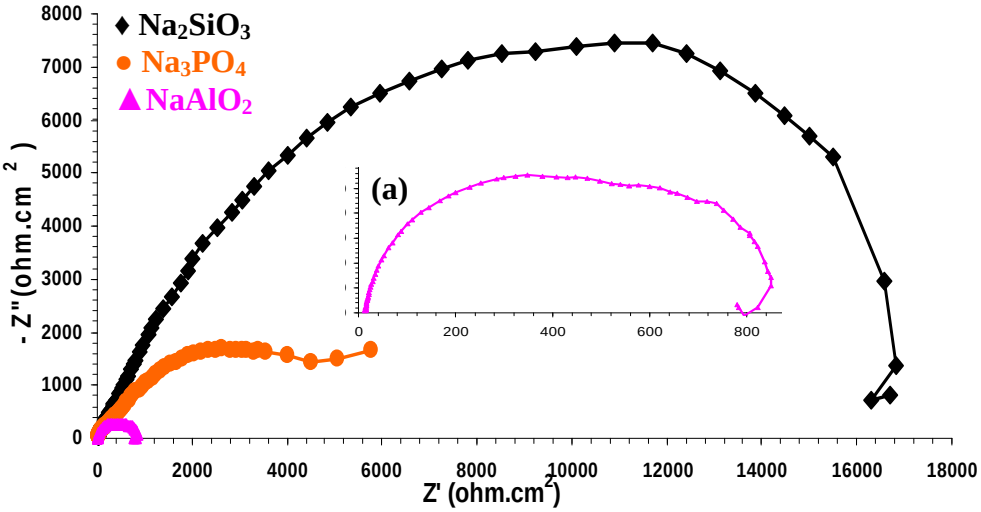

Fig. 6: Impedance curves of samples immersed in various salt solutions; (a) $NaAlO_2$ curve in large scale.

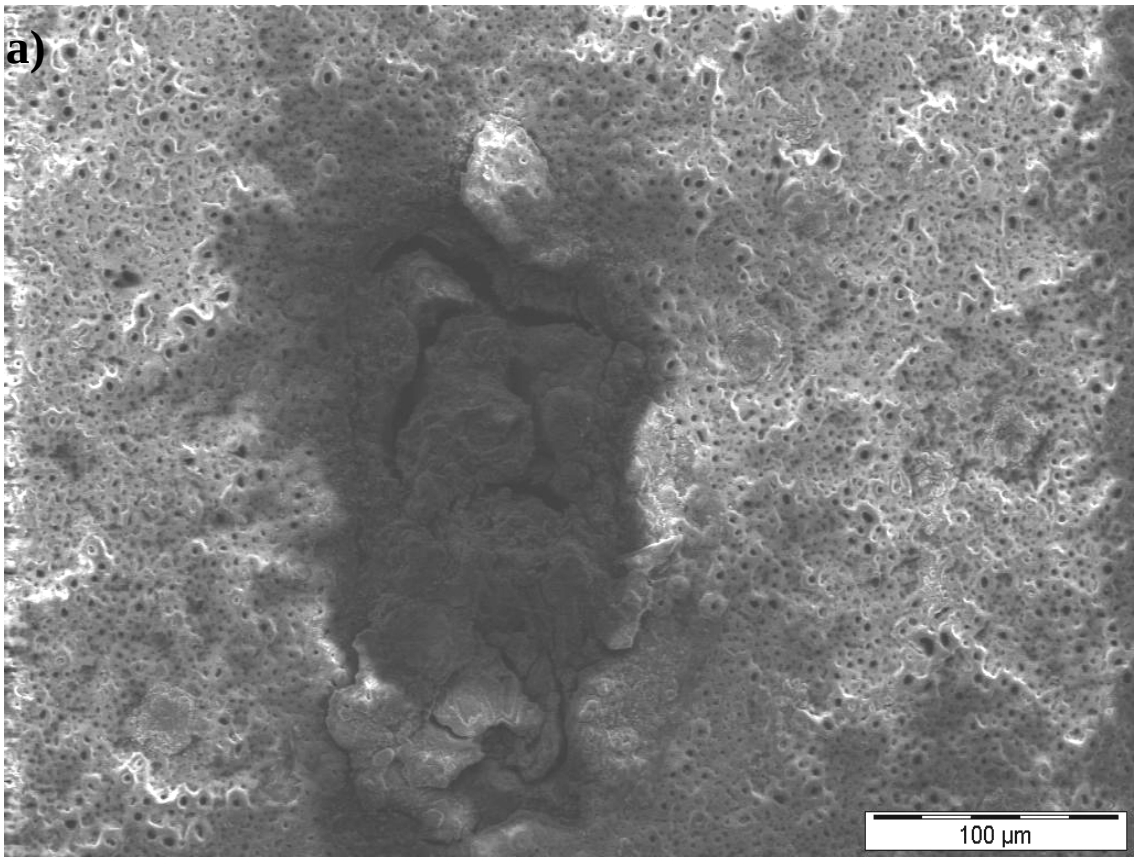
a)
100 µm

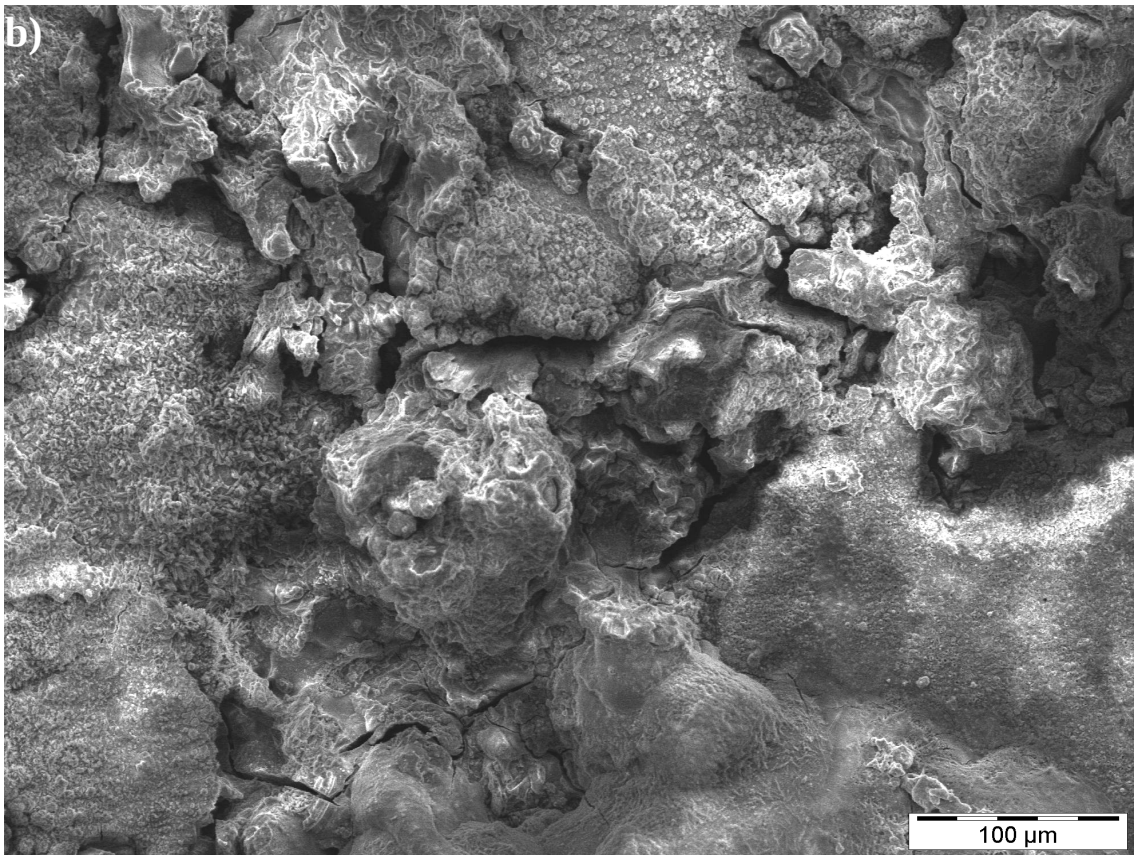
b)
100 µm

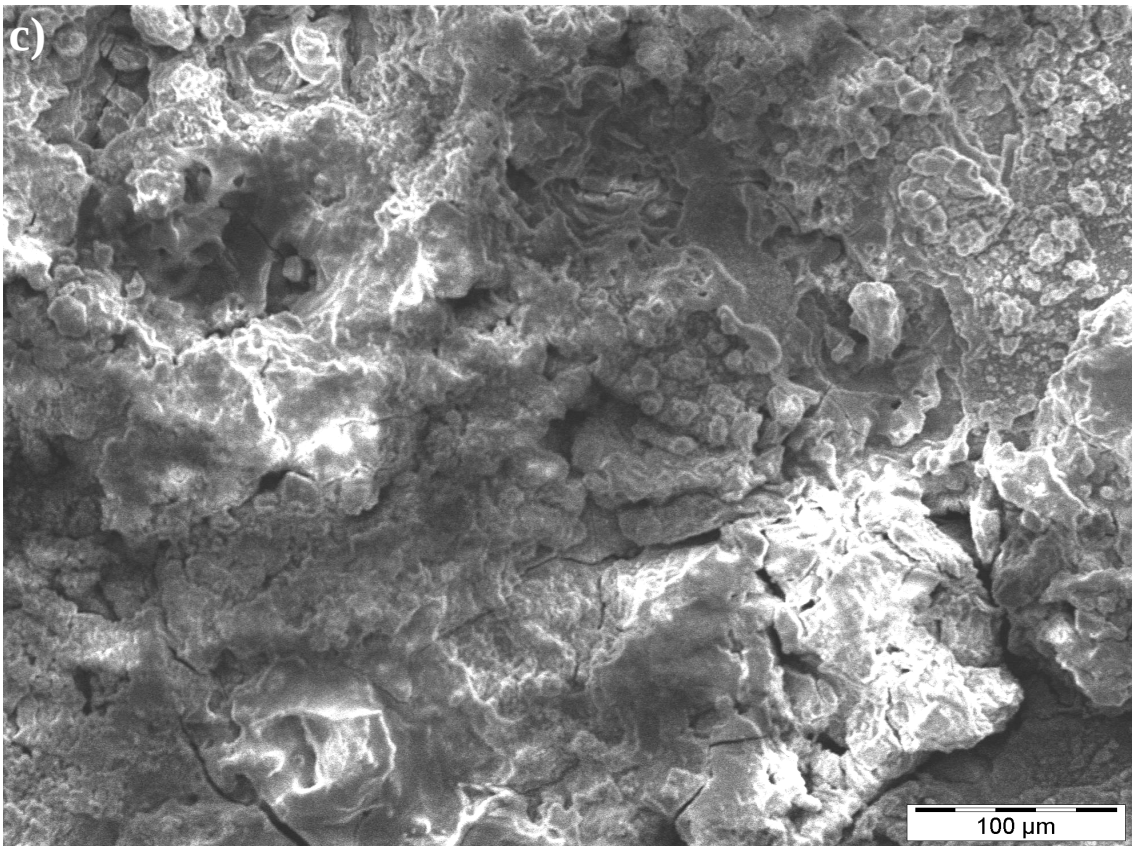

Fig. 7: Morphology of the corrosion attack of a) Na_2SiO_3+KOH, b) Na_3PO_4+KOH and c) $NaAlO_2$+KOH coatings.

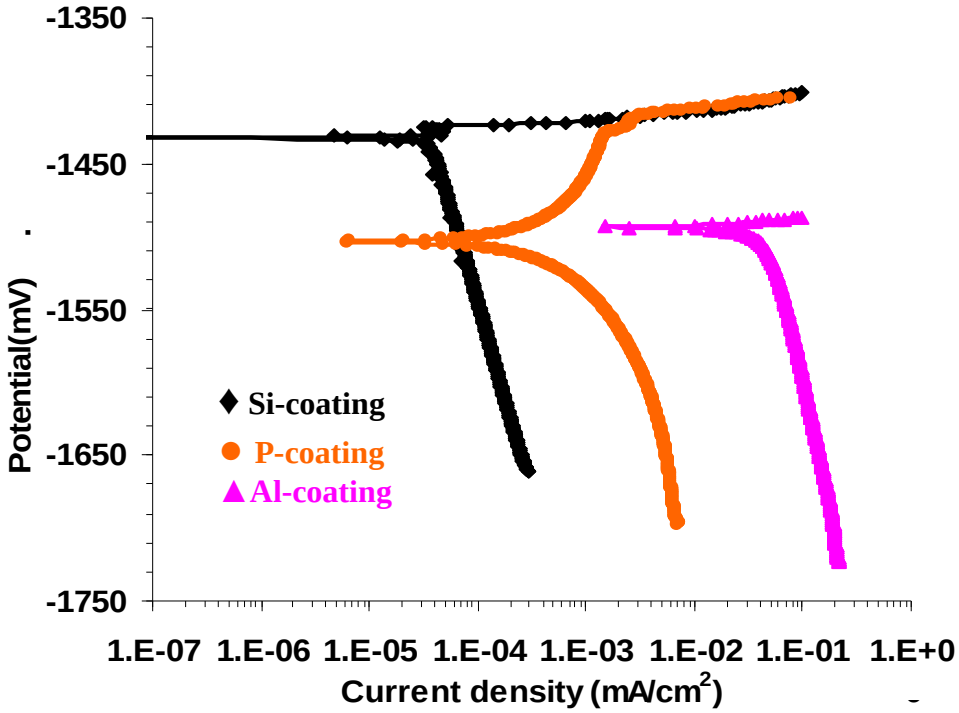

Fig. 8: Typical polarization c of three types of coatings in 3.5wt% NaCl solution; the limiting current density decreases in the order Al > P > Si.

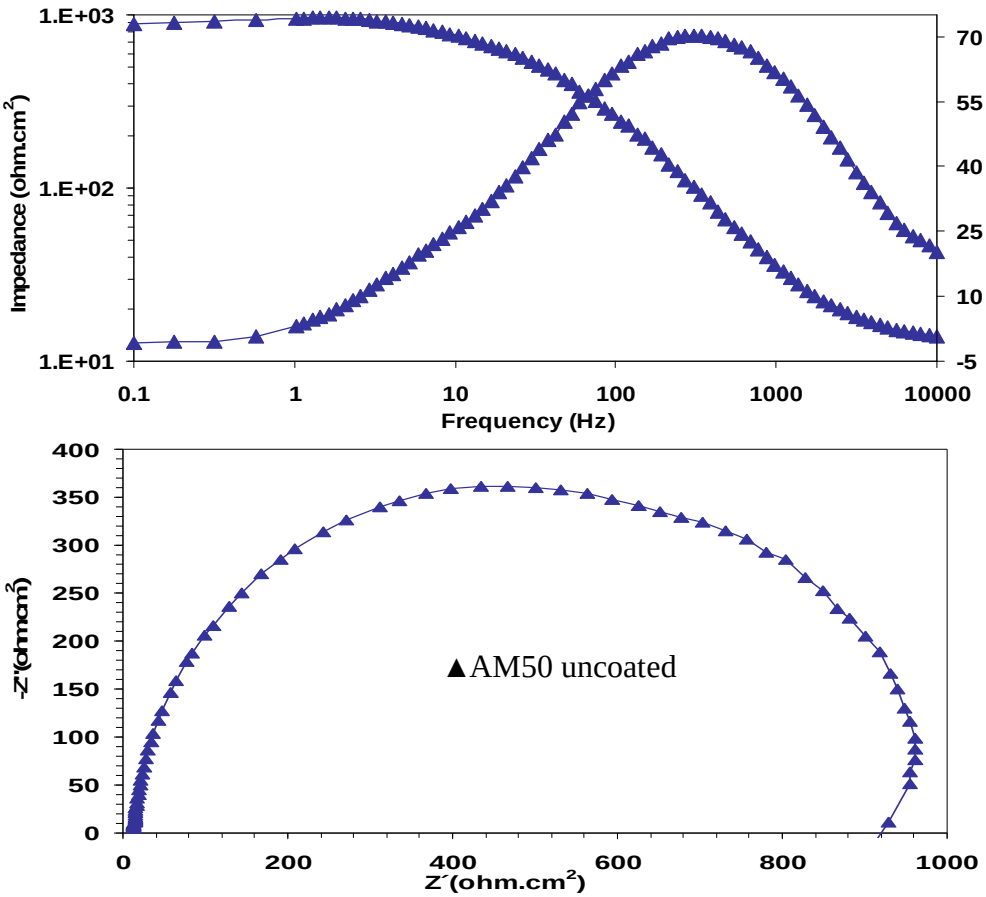

Fig. 9: Experimental results of impedance data for the uncoated AM50.

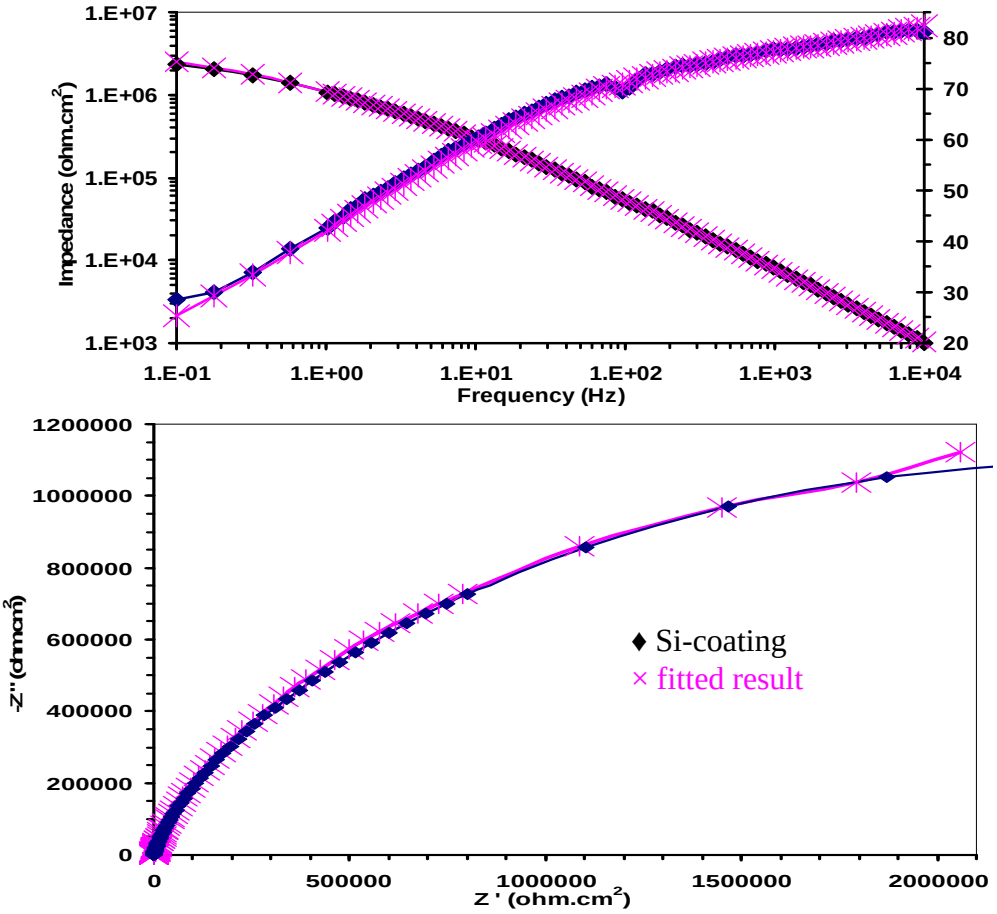

Fig. 10: Experimental and fitted results of impedance data for the Si-coating.

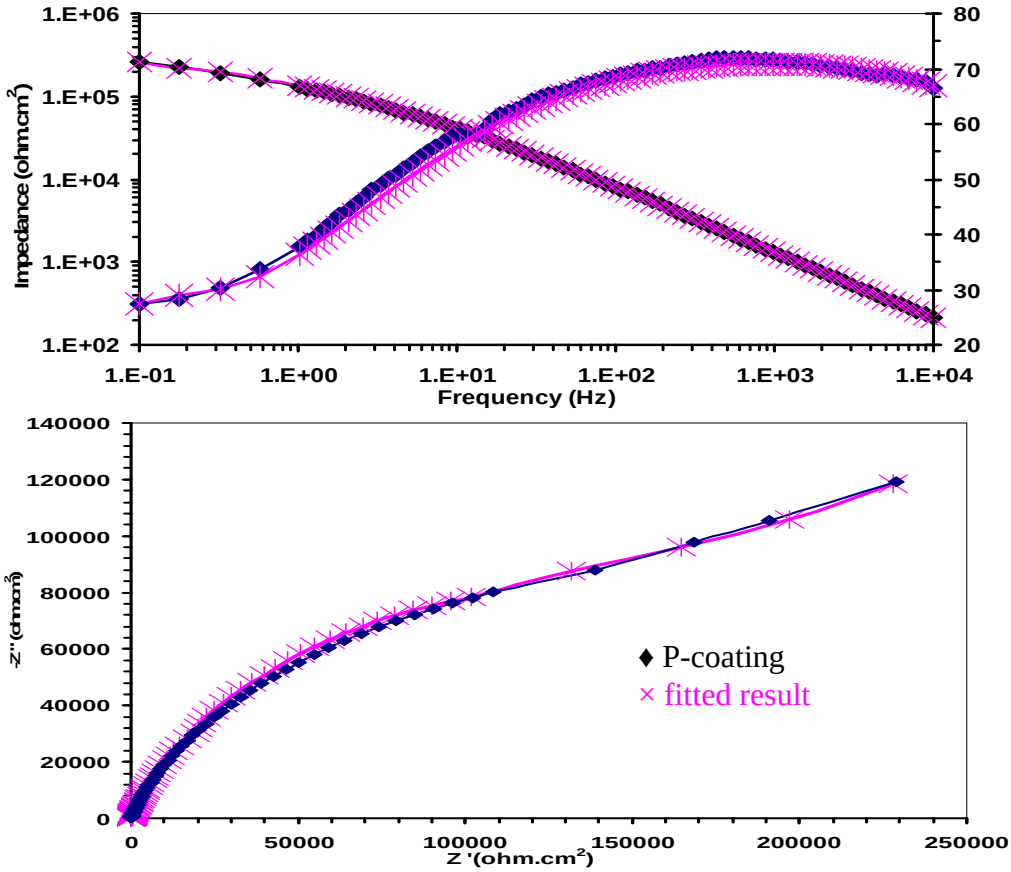

Fig. 11: Experimental and fitted results of impedance data for the P-coating.

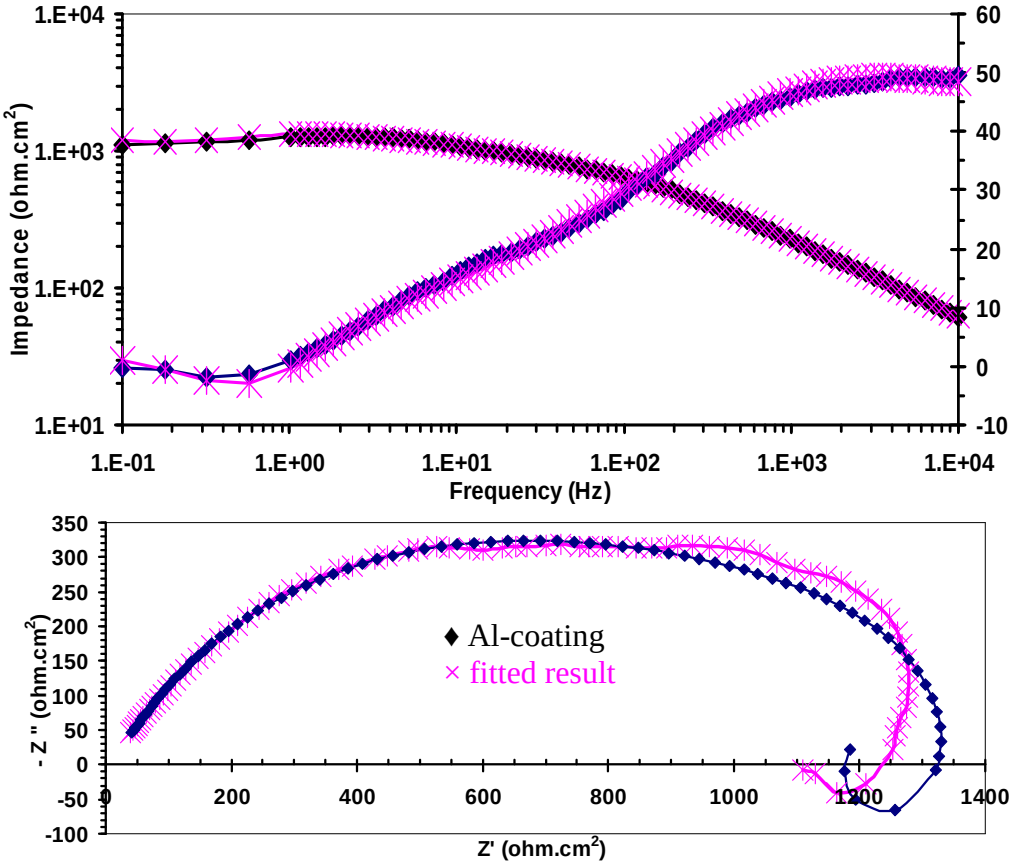

Fig. 12: Experimental and fitted results of impedance data for the Al-coating.

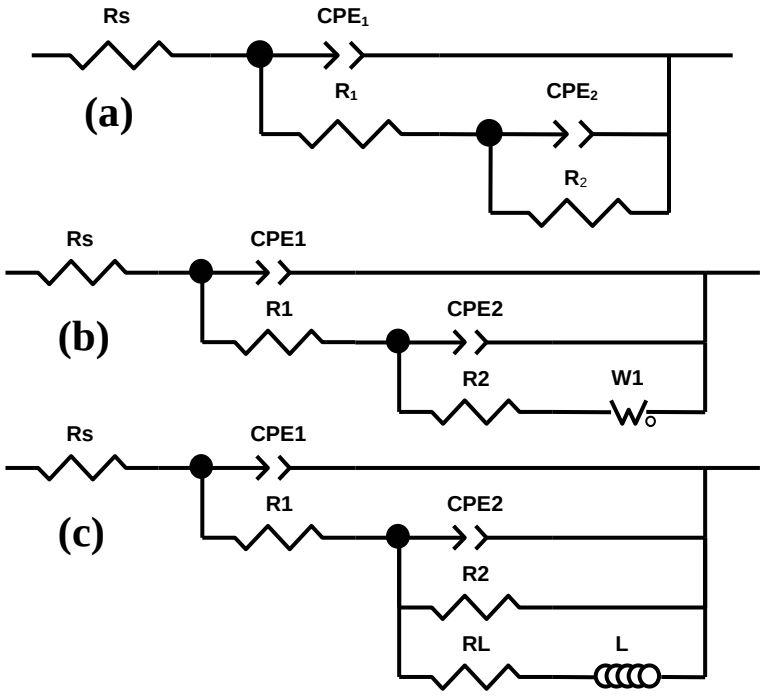

Fig. 13: Equivalent circuits for fitting the experimental data of a) Si-, b) P- and c) Al-coating.

Table 1:- Measurement of the open pores of PEO coatings

Coatings / Open pores	Si-coating	P-coating	Al-coating
% Area covered by open pores	0.5	0.7	1.6
Open pores density (pores/mm^2)	13	17	33
% Area covered by pores	3.3	1.5	3.6
pores density (pores/mm^2)	4410	31340	74450

Table 2: Polarization data for evaluating the corrosion resistance of the PEO coatings

Parameters \ Coatings	Si-coating	P-coating	Al-coating
i_{corr} (mA/cm²)	3.2×10^{-06}	9.5×10^{-04}	8.7×10^{-03}
corrosion rate (mm/year)	8.4×10^{-04}	1.3×10^{-02}	1.16

Table 3: Data of the equivalent circuits of the various coatings

coating	CPE1-P	CPE1-T	R_1	CPE2-P	CPE2-T	R_2	W1-P	W1-T	W1-R	R_L	L	Chi-Squared	Weighted Sum of Squares
Si-coating	0.89	5.19×10^{-8}	3.21×10^{4}	0.42	2.70×10^{-7}	5.64×10^{6}	-	-	-	-	-	9.9×10^{-4}	1.6×10^{-1}
P-coating	0.81	6.5×10^{-7}	6.4×10^{4}	0.44	2.2×10^{-6}	3.1×10^{5}	0.95	13.9	2.1×10^{7}	-	-	1.1×10^{-3}	1.7×10^{-1}
Al-coating	0.2	1.7×10^{-4}	2.1×10^{2}	0.71	5.4×10^{-6}	2.3×10^{3}	-	-	-	3543	1037	1.2×10^{-3}	1.9×10^{-1}